AFRL-RX-WP-TP-2010-4055

A COUPLED CREEP PLASTICITY MODEL FOR RESIDUAL STRESS RELAXATION OF A SHOT-PEENED NICKEL-BASE SUPERALLOY (POSTPRINT)

Dennis J. Buchanan and Robert A. Brockman

University of Dayton Research Institute

Reji John and Andrew H. Rosenberger

Metals Branch
Metals, Ceramics & NDE Division

JANUARY 2010

AIR FORCE RESEARCH LABORATORY
MATERIALS AND MANUFACTURING DIRECTORATE
WRIGHT-PATTERSON AIR FORCE BASE, OH 45433-7750
AIR FORCE MATERIEL COMMAND
UNITED STATES AIR FORCE

REPORT DOCUMENTATION PAGE

Form Approved
OMB No. 0704-0188

1. REPORT DATE *(DD-MM-YY)*	2. REPORT TYPE	3. DATES COVERED *(From - To)*
January 2010	Journal Article Postprint	01 January 2010 – 31 January 2010

4. TITLE AND SUBTITLE
A COUPLED CREEP PLASTICITY MODEL FOR RESIDUAL STRESS RELAXATION OF A SHOT-PEENED NICKEL-BASE SUPERALLOY (POSTPRINT)

5a. CONTRACT NUMBER
FA8650-04-C-5200

5b. GRANT NUMBER

5c. PROGRAM ELEMENT NUMBER
62102F

6. AUTHOR(S)
Dennis J. Buchanan and Robert A. Brockman (University of Dayton Research Institute)
Reji John and Andrew H. Rosenberger (AFRL/RXLM)

5d. PROJECT NUMBER
4347

5e. TASK NUMBER
RG

5f. WORK UNIT NUMBER
M02R3000

7. PERFORMING ORGANIZATION NAME(S) AND ADDRESS(ES)
University of Dayton Research Institute
Dayton, OH 45469-0020

Metals Branch (AFRL/RXLM)
Metals, Ceramics & NDE Division
Materials and Manufacturing Directorate
Wright-Patterson Air Force Base, OH 45433-7750
Air Force Materiel Command, United States Air Force

8. PERFORMING ORGANIZATION REPORT NUMBER

9. SPONSORING/MONITORING AGENCY NAME(S) AND ADDRESS(ES)
Air Force Research Laboratory
Materials and Manufacturing Directorate
Wright-Patterson Air Force Base, OH 45433-7750
Air Force Materiel Command
United States Air Force

10. SPONSORING/MONITORING AGENCY ACRONYM(S)
AFRL/RXLMN

11. SPONSORING/MONITORING AGENCY REPORT NUMBER(S)
AFRL-RX-WP-TP-2010-4055

12. DISTRIBUTION/AVAILABILITY STATEMENT
Approved for public release; distribution unlimited.

13. SUPPLEMENTARY NOTES
Journal article published in the *Journal of Metals* (*JOM*), Vol. 62, No. 1 (2010). PAO Case Number: 88ABW-2009-3831; Clearance Date: 02 Sep 2009. The U.S. Government is joint author of this work and has the right to use, modify, reproduce, release, perform, display, or disclose the work.

14. ABSTRACT
Shot peening is a commonly used surface treatment process that imparts compressive residual stresses into the surface of metal components. Compressive residual stresses retard initiation and growth of fatigue cracks. During component loading history, shot-peened residual stresses may change due to thermal exposure, creep, and cyclic loading. In these instances, taking full credit for compressive residual stresses would result in a nonconservative life prediction. This article describes a methodical approach for characterizing and modeling residual stress relaxation under elevated temperature loading, near and above the monotonic yield strength of IN100. The model incorporates the dominant creep deformation mechanism, coupling between the creep and plasticity models, and effects of prior plastic strain to simulate surface treatment deformation.

15. SUBJECT TERMS
shot peening, compressive residual stresses, thermal exposure, creep, cyclic loading

16. SECURITY CLASSIFICATION OF:			17. LIMITATION OF ABSTRACT:	18. NUMBER OF PAGES	19a. NAME OF RESPONSIBLE PERSON (Monitor)
a. REPORT	b. ABSTRACT	c. THIS PAGE			Reji John
Unclassified	Unclassified	Unclassified	SAR	12	19b. TELEPHONE NUMBER *(Include Area Code)* N/A

Standard Form 298 (Rev. 8-98)
Prescribed by ANSI Std. Z39-18

A Coupled Creep Plasticity Model for Residual Stress Relaxation of a Shot-peened Nickel-based Superalloy

Dennis J. Buchanan, Reji John, Robert A. Brockman, and Andrew H. Rosenberger

Shot peening is a commonly used surface treatment process that imparts compressive residual stresses into the surface of metal components. Compressive residual stresses retard initiation and growth of fatigue cracks. During component loading history, shot-peened residual stresses may change due to thermal exposure, creep, and cyclic loading. In these instances, taking full credit for compressive residual stresses would result in a nonconservative life prediction. This article describes a methodical approach for characterizing and modeling residual stress relaxation under elevated temperature loading, near and above the monotonic yield strength of IN100. The model incorporates the dominant creep deformation mechanism, coupling between the creep and plasticity models, and effects of prior plastic strain to simulate surface treatment deformation.

INTRODUCTION

Compressive residual stresses retard crack initiation and growth, resulting in improved fatigue performance. Numerous studies[1–7] on steels, titanium, and nickel-based superalloys have shown that residual stresses generated via surface treatment relax when subjected to elevated temperature exposure or mechanical loading. A variety of sophisticated empirical models have been developed and shown to capture trends in residual stress relaxation.[3,4,7] However, material microstructure, hardening behavior, plastic strain, and the underlying physical deformation mechanisms responsible for stress relaxation are not incorporated into many of these models. The result is a relaxation model that must be recalibrated for each surface treatment process and associated control parameters. Selecting a relaxation model that reflects the proper deformation mechanism provides for reliable predictions that rely less on calibration and fine-tuning of model parameters for each application.

CREEP DEFORMATION MECHANISMS AND MODELS

The primary variables associated with creep deformation and creep rate are stress, temperature, and time. Much of the early work characterizing creep behavior was aimed at fitting empirical equations as a function of stress, temperature, and time. Furthermore, it is typically assumed that these equations are products separable into functions for stress and temperature.

A major element missing from the empirical creep models is the evolution of material microstructure with time or deformation history. It is almost always assumed that microstructure, and hence the material properties remain unchanged throughout the deformation history. Aspects of material microstructure such as grain size, dislocation structure, inclusions, vacancies, etc., all have an impact on the deformation rate. Both time-hardening and strain-hardening approaches are suitable if the creep rate is dominated by a single deformation mechanism. If multiple deformation mechanisms are active, or the dominant mechanism changes with thermal and mechanical loading history, simple time- and strain-hardening approaches fail to capture the loading response. Schoeck[8] presents a more general formulation for creep rate that accounts for multiple independent creep mechanisms which addresses the evolution of a changing microstructure as a contributing factor to the creep rate, but implies the deformation mechanisms are independent.

Numerous models have been developed for the dominant creep mechanisms such as glide and climb of dislocations, and diffusion through grains and along grain boundaries. Nowick and Machlin[9] and Weertman[10] developed the early dislocation creep models to describe climb and glide deformation mechanisms which gave rise to many of the commonly used exponential and hyperbolic sine formulations for creep rate. The interaction or competition between deformation mechanisms can become

How would you...

...describe the overall significance of this paper?

This paper describes a coupled creep and plastic deformation model for relaxation of residual stresses that incorporates both the initial residual stress and plastic strain depth profiles into the solution. The applicability of the model is demonstrated on a shot peened nickel-based superalloy subject to thermomechanical loading. Model predictions are validated with measured x-ray diffraction residual stress depth profiles.

...describe this work to a materials science and engineering professional with no experience in your technical specialty?

A constitutive material model based on a dislocation creep deformation mechanism coupled with a rate-independent plasticity model was developed to predict the relaxation of residual stresses in nickel-base superalloys under elevated temperature loading conditions.

...describe this work to a layperson?

A mathematical model that implements the known material deformation behavior was developed to predict the evolution of internal residual stresses of manufactured components made from metallic materials that are subject to applied mechanical and temperature loading histories.

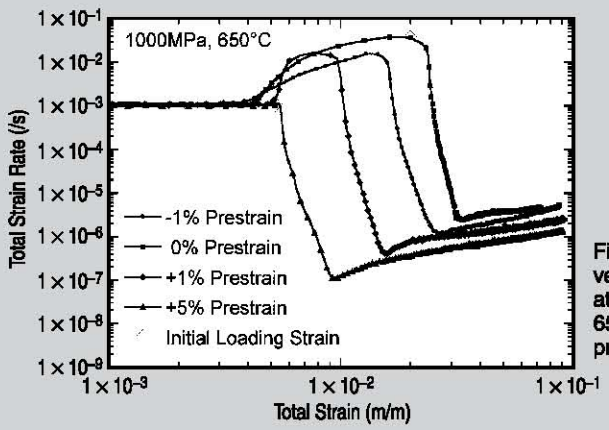

Figure 1. Total strain rate versus total strain for IN100 at σ_{max} = 1,000 MPa and 650°C for different levels of prestrain.

complex. Initial approaches to represent material degradation under creep loading include the continuum damage mechanics (CDM) approaches of Kachanov[11] and Rabotnov[12] that incorporate a single damage parameter and associated evolution equation. More recently, the simple damage parameters in the CDM approach have been replaced by specific degradation models representing mechanisms such as cavity nucleation and growth, subgrain coarsening, multiplication of mobile dislocations, and thermally and environmentally driven mechanisms.[13–19]

A number of modeling approaches have been developed to account for the combined contributions of plasticity and creep.[13–15,20–24] The trend has been to incorporate plasticity and creep into a single unified inelastic model. These models have evolved to include complex nonlinear hardening rules to capture the Bauschinger effect, and cyclic hardening or softening. Unfortunately, the microstructural deformation mechanisms behind creep and plastic deformation, which are fundamentally different, have been combined in this approach.

RELAXATION OF SHOT-PEENED RESIDUAL STRESSES

Shot peening has been employed for decades to impart compressive residual surface stresses for retardation of crack initiation and crack growth. Numerous studies have characterized the beneficial effects of compressive residual surface stresses on fatigue life for metallic materials.[1–7] For applications that utilize aluminum and titanium alloys, subjected to moderate temperatures and stresses, residual stresses are assumed to be stable with repeated cyclic stress-controlled loading. In contrast, nickel-base superalloys are typically selected for applications where temperatures may reach 80 percent of the melting temperature, and stresses approach or exceed the monotonic yield strength. At elevated temperatures and high stress loading conditions, inelastic deformation will alter the original residual stress depth profile. Furthermore, changes to the microstructure resulting from shot peening, long term elevated temperature exposure, and deformation history may accelerate the relaxation rate of residual stresses. Understanding the relaxation of residual stresses is necessary to improve the ability to predict service life of shot-peened components.

Thermal relaxation studies on shot-peened steels,[4] titanium alloys,[1] and nickel alloys[1–3,5,6] have demonstrated that relaxation of residual stresses may occur at relatively low temperatures and over short durations. Research into relaxation of residual stresses subject to mechanical loading has followed a much different path than thermal relaxation. For thermal relaxation, temperature and exposure time are the primary parameters, while for mechanical relaxation the important factors are temperature, maximum and minimum applied stress, loading frequency, hold time, waveform shape, and number of applied cycles.

See the sidebar for experimental details.

COUPLED CREEP-PLASTICITY MODEL

The constitutive model developed in this study is based on a rate-independent plasticity model, and a strain-hardening creep model that is coupled to the plasticity model through the plastic strain rate and yield surface size. The plasticity model is based on the von Mises

EXPERIMENTAL INVESTIGATION

IN100 is a powder metal (PM) nickel-based superalloy with an average grain size of approximately 25 μm. The microstructure is composed of a continuous gamma (γ) matrix, and precipitate cubical gamma prime (γ'). The cubical gamma prime is responsible for the excellent creep resistance of this alloy. The gamma prime is strong and ductile which limits dislocation interaction and movement through the microstructure. Additional details about the baseline microstructure are described in the literature.[25]

The effect of room-temperature plastic prestrain on creep deformation behavior is shown in Figure 1 for an applied stress of 1,000 MPa and temperature of 650°C. This figure is a plot of total strain rate versus total strain for the entire elevated temperature loading history. The effect of room-temperature prestrain, which is used to simulate surface treatment, clearly affects the elastic, plastic, and creep response at elevated temperature. The zero percent prestrain case is the baseline case for comparison. The deformation history starts by elastic loading at a constant strain rate of 1.0×10^{-3} /s followed by yielding, which produces plastic deformation and an increase in the total strain rate until reaching the target stress, after which the strain rate drops off during primary creep deformation. The creep strain rate reaches a minimum and then increases transitioning to tertiary creep. The one percent prestrain case exhibits delayed yielding resulting from an increase in the yield surface during room-temperature prestrain loading. The minus one percent prestrain loading exhibits a lower tensile yield resulting from the Bauschinger effect and supports the need to include a plasticity model with kinematic hardening. Also, the increase in strain rate is more gradual for the compressive prestrain, which is consistent with the more gradual hardening curve often observed in cyclic hardening. Only for the five percent prestrain case is yielding mitigated upon loading to 1,000 MPa. The data also show that any prestrain, tensile or compressive, results in a decrease in the minimum strain rate. The open diamond symbols represent the initial loading strain, and clearly reflect the complex deformation that occurs prior to reaching the target stress for creep.

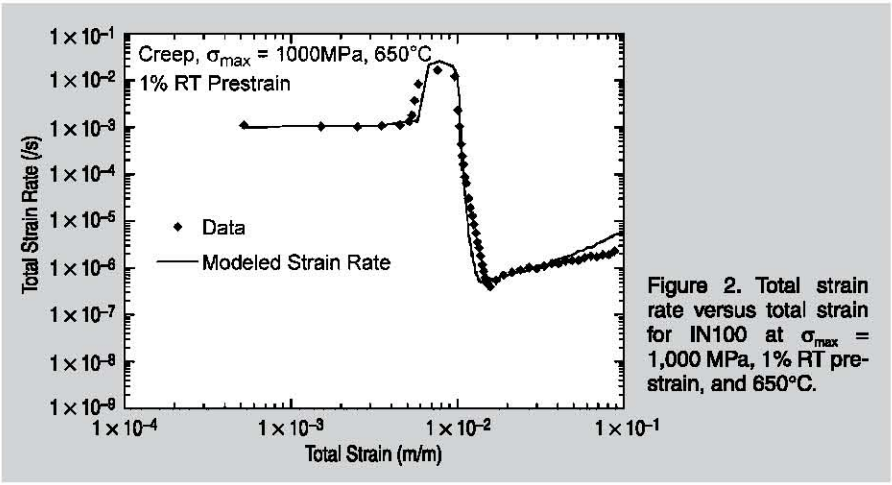

Figure 2. Total strain rate versus total strain for IN100 at σ_{max} = 1,000 MPa, 1% RT prestrain, and 650°C.

effective stress with a nonlinear mixed isotropic-kinematic hardening rule as described by Dodds.[26] The creep model follows the physics-based modeling of dominant deformation mechanisms similar to the approaches of Dyson, McLean, and others.[16–19] Based on the scanning electron microscopy (SEM) and transmission electron microscopy (TEM) observations of the shot-peened and thermally exposed microstructure, it has been argued that the microstructure remains stable over the range of temperatures and exposure times in this study. Therefore a microstructural model dominated by a single deformation mechanism is sufficient to model residual stress relaxation behavior. The elastic-plastic-creep model is cast in an implicit integration form suitable as a standard user material subroutine (UMAT) for implementation into ABAQUS/Standard.

Identification of the primary creep deformation mechanism is required before development of a model may begin. One approach to determining the dominant mechanism is to fit the minimum creep rate versus stress data to a power law equation and evaluate the exponent of stress (n). Bulk diffusion through the grain (Nabarro–Herring Creep) and diffusion along grain boundaries (Coble Creep) may be characterized by minimum creep rates that are directly proportional to stress raised to an exponent n = 1. Dislocation creep mechanisms typically have a power law exponent that is higher and with a range of n = 3–6. The creep rate data from this study exhibit an exponent of $n \approx 6$, and therefore dislocation creep motion is the primary deformation mechanism for the range of conditions evaluated. Therefore, a creep model with dislocation creep as the dominant deformation mechanism is chosen for this alloy and range of operating conditions.

The development of the creep model follows the microstructurally based deformation mechanism approach of McLean and Dyson.[16] The basic model is adapted to incorporate the effects of prior plastic strain and coupling to the plasticity model. The 1D effective creep strain rate relation, based on dislocation creep as the dominant deformation mechanism, is defined such that it is identical to the axial component under uniaxial loading,

$$\dot{\bar{\varepsilon}}^{c} = \dot{\varepsilon}_{o}\left(1+\bar{\varepsilon}^{dm}\right)\sinh\left(\frac{\sigma-\alpha}{\sigma_{\kappa}\kappa}\right) \quad (1)$$

where

$\dot{\bar{\varepsilon}}^{c}$ = effective creep strain rate,

$\dot{\varepsilon}_{o}$ = creep strain rate parameter,

$\bar{\varepsilon}^{dm}$ = effective mobile dislocation density,

σ = applied stress,

α = back stress,

σ_{κ} = normalized stress parameter (nondimensional),

κ = size of yield surface.

The microstructural evolution equation for multiplication of mobile dislocations has been modified to incorporate the effect of plastic strain rate as follows:

$$\dot{\bar{\varepsilon}}^{dm} = M\dot{\bar{\varepsilon}}^{p} + N\dot{\bar{\varepsilon}}^{c} \quad (2)$$

Parameters M and N are coefficients that determine the contributions of plastic strain rate and creep rate toward the increase in dislocation mobility, respectively. This is a strain-induced form of damage that increases with increasing strain rate. In the absence of plastic strain, Equation 2 reduces to the creep damage rate equation described by McLean and Dyson.[16] Details of the constitutive equations and solution procedure are described elsewhere.[27,28]

VALIDATION OF MODEL

The coupled creep-plasticity model has been calibrated using creep data with prior plastic strain as described in the Experimental Investigation section. A one dimensional model of the constitutive equation has been developed as an expedient method to determine the constitutive parameters and associated confidence limits. The parameters deduced from tensile, creep, and cyclic tests fit to the one-dimensional form of the coupled creep-plasticity model have been implemented into a three-dimensional finite element material model.

Overall, the coupled creep-plasticity model captures the effects of prior plastic strain, plastic strain during loading,

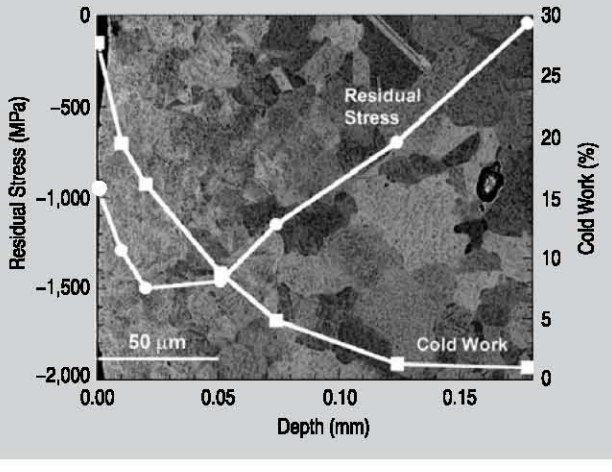

Figure 3. Composite of baseline residual stress and cold work depth profiles overlaid on shot-peened microstructure.

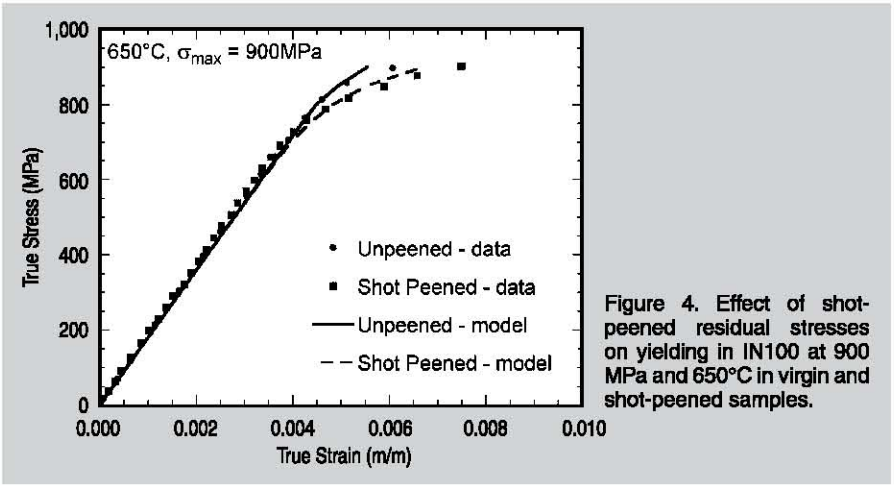

Figure 4. Effect of shot-peened residual stresses on yielding in IN100 at 900 MPa and 650°C in virgin and shot-peened samples.

and applied stress level on the creep deformation response. For example, Figure 2 incorporates both room-temperature plastic prestrain ($\varepsilon_p = 1$ %) and plastic strain during elevated-temperature loading to the target stress of $\sigma = 1{,}000$ MPa. The model captures the delayed yielding during loading resulting from the increase in the yield surface from room-temperature prestrain loading and the sharp increase in strain rate associated with yielding under stress-controlled loading. Furthermore, the creep response including the minimum creep rate is accurately captured by the model.

APPLICATION OF MODEL

The proposed coupled creep-plasticity model has been shown to be capable of reproducing material responses over complex loading histories in which inelastic prestrain affects the subsequent creep behavior rather dramatically. This section considers the analysis of relaxation of shot-peened residual stresses in IN100 subjected to mechanical loading. Model predictions corresponding to residual stress relaxation of shot-peened dogbone specimens are presented to demonstrate the effectiveness of the proposed coupled model for problems involving sharp spatial gradients, such as those encountered in shot-peened components.

After identifying limiting factors such as material availability, size of test matrix, and experimental and analytical requirements, a dogbone specimen with a rectangular cross section (2 mm thick × 10 mm wide) was chosen for the shot-peening geometry. A large flat shot-peened surface is desired to maximize the size of the irradiated region during x-ray diffraction (XRD). Based on residual stress depth profiles on a similar superalloy, IN718,[5] and typical shot-peening specifications for turbine engine components, an Almen intensity of 6A has been selected. The residual stress measurements were collected at the surface and at nominal depths of 0.012, 0.025, 0.050, 0.075, 0.125, 0.175, 0.250, and 0.350 mm. Characterization of the initial residual stress and plastic strain depth profiles are necessary for accurate prediction of the evolution of stresses and plastic strains under applied thermal and mechanical loading. Figure 3 is a backscatter SEM micrograph of a polished cross section of IN100. The left side of the image is the shot-peened surface of the sample. The left 50 μm area shows a distinct change in microstructure resulting from the shot-peening-induced deformation. The right side shows the interior, with a typical representation of the microstructure and individual grains. Superimposed over the microstructure are representative residual stress and percent cold work (plastic strain) depth profiles determined by XRD.

Although the volume of deformed material is small, the presence of the residual stresses is sufficient to affect the deformation response in the test specimens. Validation of the model with residual stresses is shown in the stress versus strain response of Figure 4. The figure shows the experimental data and model predictions, respectively, from an unpeened cylindrical dogbone specimen and a shot-peened flat dogbone specimen. The model captures the lower yield point in the shot-peened specimen that is observed in the experimental results. Note that these are average stresses throughout the specimen. Thus, deviation from the unpeened sample shows that yielding occurs at the interior of the shot-peened sample which started at a tensile residual stress. The results describe the effect of residual stress on the deformation response of the test specimens. Further validation of the coupled creep plasticity model is accomplished by comparing the measured retained residual stress depth profile after loading with model predictions.

Prediction for retained residual stresses for a single mechanical loading cycle is shown in Figure 5. The maximum applied stress of 900 MPa results in yielding during loading. The room-temperature (RT) baseline residual stress profile is an average of six profiles. This is the residual stress profile used as the initial conditions in the finite element model. Three specimens, tested under these loading conditions, are averaged and shown as a solid line representing the mean response with error bars displaying the range of the XRD measurements for the axial resid-

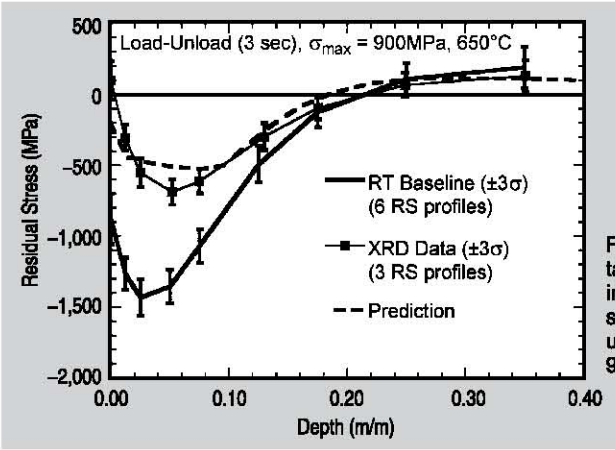

Figure 5. Prediction for retained residual stresses in shot-peened dogbone specimen from single load-unload cycle in IN100 at 900 MPa and 650°C.

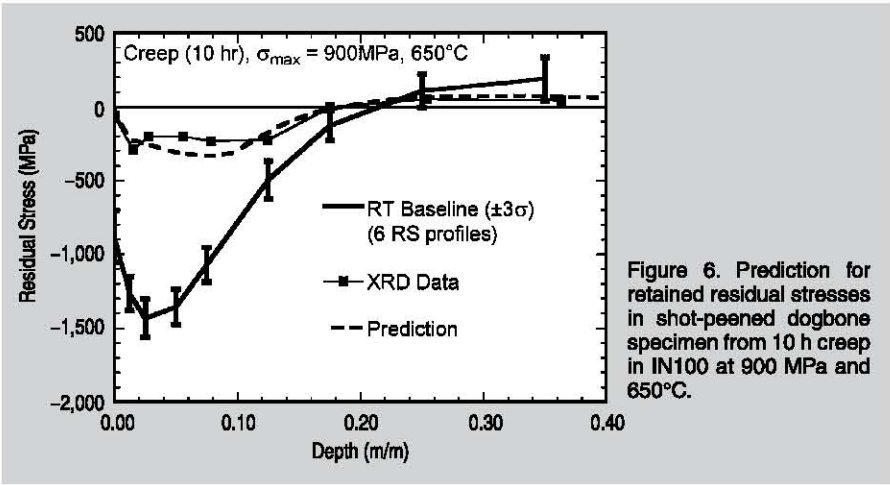

Figure 6. Prediction for retained residual stresses in shot-peened dogbone specimen from 10 h creep in IN100 at 900 MPa and 650°C.

ual stress profile. The range in the XRD measurements is greatest in the region where the residual stress profile has the largest value of compressive residual stress. This is expected since the errors in depth measurement, and stress correction for material removal, are greatest in the shallow depth region. The prediction for the residual stress profiles, shown as a thick dotted line without symbols, captures the residual stress relaxation trend. Surprisingly, the data displays a small tensile surface residual stress. It has been demonstrated in the literature[29] that gross plastic straining of the entire cross section of a shot-peened test specimen can reverse the residual stress profile such that tensile residual stresses develop on the surface with compression in the center.

Prediction for the retained residual stresses under sustained load (creep) loading, for 10 hours, is shown in Figure 6. The prediction captures the surface residual stress and peak compressive stress. Sustained loading is more detrimental than the load-unload cycle to retained compressive residual stresses for applied stresses that develop plastic strain during loading. Furthermore, sustained loading continues to relax residual stresses with increasing creep time.

Although significant relaxation of compressive residual stresses occurs during creep relative to that of the load-unload cycle, the surface residual stress remains compressive. This is relatively surprising since analysis of the creep strain data for the 10 hour creep test revealed that the specimen was in tertiary creep and close to failure when the test was stopped.

CONCLUSIONS

A coupled creep-plasticity model that incorporates plastic strain and yield surface state variables has been developed that reflects the correct dominant deformation mechanism identified for relaxation of shot-peened residual stresses in this alloy. The coupled creep-plasticity approach facilitates incorporation of other creep deformation mechanisms into the model without additional extensive experimental testing and calibration. Although the applied loading conditions were intentionally chosen to promote yielding and thermal relaxation for this study, a significant portion of the original compressive surface residual remains after loading to retard initiation and growth of fatigue cracks. The model has been validated and shown to capture the complex deformation history with prior room-temperature prestrain. The model successfully captured the effects of residual stress on deformation history and the retained residual stress profile for different loading histories.

ACKNOWLEDGEMENTS

This work was performed at the Air Force Research Laboratory, Materials and Manufacturing Directorate, Wright-Patterson Air Force Base, OH 45433-7817 under on-site contract no. FA8650-04-C-5200.

References

1. P. Prevéy, D. Hornbach, and P. Mason, *Proceedings of the 17th Heat Treating Society Conference and Exposition and the 1st International Induction Heat Treating Symposium,* ed. D.L. Milam et.al. (Materials Park, OH: ASM International, 1998), pp. 3–12.
2. T.P. Gabb et al., *TMS Letters,* 1 (5) (2004), pp. 115–116.
3. W. Cao et al., *Material Science and Technology,* 10 (November 1994), pp. 947–954.
4. H. Holzapfel et al., *Material Science and Engineering,* A248 (1998), pp. 9–18.
5. P. Prevéy, *Proceedings of the 20th ASM Materials Solution Conference & Exposition* (Materials Park, OH: ASM International, 2000), pp. 426–434.
6. D.J. Buchanan, R. John, and N.E. Ashbaugh, *ASTM STP 1497 - Residual Stress Effects on Fatigue and Fracture Testing and Incorporation of Results into Design* (West Conshohocken, PA: ASTM, 2007), pp. 47–57.
7. J.L. Chaboche and O. Jung, *International Journal of Plasticity,* 13 (10) (1998), pp. 785–807.
8. G. Schoeck, *Mechanical Behavior of Materials at Elevated Temperatures,* ed. J.E. Dorn (New York: McGraw-Hill Book Company, Inc., 1961), pp. 79–107.
9. A.S. Nowick and E.S. Machlin, *National Advisory Committee for Aeronautics (NACA), Technical Note No. 1039* (Washington, D.C.: NACA, April 1946). [NACA was dissolved on October 1, 1958 and its assets transferred to the newly created National Aeronautics and Space Administration (NASA).]
10. J. Weertman, *J. Applied Physics,* 26 (10) (1955), pp. 1213–1217.
11. L.M. Kachanov, *Izv. Akad. Nauk. SSR, Otd Tekh., Nauk No. 8* (1958), pp. 26–31.
12. Y.N. Rabotnov, *Creep Problems in Structural Members* (New York: American Elsevier Publishing Co., 1969), p. 137.
13. J.L. Chaboche, *J. Applied Mechanics,* 55 (March 1988), pp. 59–64.
14. J.L. Chaboche, *J. Applied Mechanics,* 55 (March 1988), pp. 65–72.
15. D.R. Sanders (Ph.D. thesis, Texas A&M University, 1986).
16. M. McLean and B.F. Dyson, *J. Engineering Materials and Technology,* 122 (July 2000), pp. 273–278.
17. B.F. Dyson, *J. Pressure Vessel Technology,* 122 (August 2000), pp. 281–296.
18. S.K. Sondhi, B.F. Dyson, and M. McLean, *Acta Materialia,* 52 (2004), pp. 1761–1772.
19. H. Basoalto et al., *Superalloys 2004,* ed. K.A. Green et al. (Warrendale, PA: TMS, 2004), pp. 897–906.
20. S.R. Bodner, *J. Applied Mechanics,* Transactions of the ASME (June 1975), pp. 385–389.
21. K. Walker, *NASA Contractor Report, NASA-CR-165533* (Springfield, VA: National Technical Information Service, 1981).
22. V.G. Ramaswamy, *NASA Contractor Report 3998* (Washington, D.C.: NASA Scientific and Technical Information Branch, 1986).
23. D.N. Robinson, *ORNL TM-5969* (Oak Ridge, TN: U.S. Department of Energy Technical Information Center, 1978).
24. A.K. Miller, *Trans. ASME Journal of Engineering Materials and Technology,* 96 (1976), p. 97.
25. K. Li, N.E. Ashbaugh, and A.H. Rosenberger, *Superalloys 2004,* ed. K.A. Green et al. (Warrendale, PA: TMS 2004), pp. 251–258.
26. R.H. Dodds, *Computers & Structures,* 26 (5) (1987), pp. 767–779.
27. D.J. Buchanan et al., *Superalloys 2008,* ed. R.C. Reed et al. (Warrendale, PA: TMS 2008), pp. 965–974.
28. D.J. Buchanan, R. John, and R.A. Brockman, *J. Engineering Materials and Technology,* 131 (3) (2009), 031008.
29. D. Kirk, *Proceedings of the Third International Conference on Shot Peening,* ed. H. Wohlfahrt, R. Kopp, and O. Vöhringer (Mishawaka, IN: Int'l. Scientific Committee for Shot Peening, 1987), pp. 213–220.

Dennis J. Buchanan, Reji John, Robert A. Brockman, and Andrew H. Rosenberger are with the Materials and Manufacturing Directorate, Air Force Research Laboratory, Wright-Patterson Air Force Base, OH 45433-7817. Buchanan and Brockman are also with the University of Dayton Research Institute, Dayton, OH 45469-0020. Dr. Buchanan can be reached at dennis.buchanan@wpafb.af.mil.